Methanol Promoted Oxidation of Nitrogen Oxide (NO_x) by Encapsulated Ionic Liquids (ENILs)

Rubén Santiago[1*], Susanne Mossin[2], Jorge Bedia[1], Rasmus Fehrmann[2], and José Palomar[1]

[1]*Chemical Engineering Department. Universidad Autónoma de Madrid. 28049 Madrid. Spain*

[2]*Centre for Catalysis and Sustainable Chemistry, Department of Chemistry, Technical University of Denmark, DK-2800 Kgs. Lyngby (Denmark).*

Corresponding author: ruben.santiago@uam.es

Keywords: NO oxidation; NO_x removal; Ionic Liquids; ENIL; Flue gas

Abstract

The removal of nitrogen oxides (NO_x) has been extensively studied due to their harmful effects to health and environment. In this work, Encapsulated Ionic Liquids (ENILs) are used as catalysts for the NO oxidation at humid conditions and low temperatures. Hollow carbon capsules (C_{Cap}) were first synthetized to contain different amounts of 1-butyl-3-methylimidazolium nitrate IL ([bmim][NO_3]), responsible for the catalytic oxidation. Then, the materials were characterized using different techniques, by analyzing microstructure, porosity, elemental composition and thermal stability. The catalytic performance of ENIL materials was tested for NO conversion at different conditions. Thus, NO concentration was fixed at 2,000 ppm at dry and humid conditions. Then, the methanol promotion of the reaction was demonstrated, increasing the NO conversion values in all cases, and the alcohol/water ratio was optimized. The temperature effect was studied as well, using the optimal conditions based on the previous measurements. The results reflect that humid conditions do not have a negative effect in terms of NO conversion when using ENILs, opposite behavior as the observed for C_{Cap} and traditional catalysts studied before. Low amount of IL inside the material (40% in mass) was found to be the optimum for the task, reaching conversions of almost 45% in near industrial conditions of temperature and O_2 and H_2O concentrations in the flue gas with a GHSV = 10,000 h^{-1}.

Introduction

Nitrogen oxides (NO_x) are one of the major air pollutants from traditional electrical production as fossil fuel combustion, leading to well-known harmful effects [1, 2]. These negative effects comprise not only to the human health, causing important respiratory problems [3], but also atmospheric pollution by acid rain, photochemical smog and ozone layer depletion [4, 5]. The major constituents of NO_x are nitrogen dioxide (NO_2) and nitric oxide (NO), which is an intermediate of the nitric acid synthesis in the chemical industry. Due to the low solubility of this gas in traditional solvents [6], it is attractive to develop systems to remove or convert this compound into value-added or not harmful products. The most important technologies of the chemical industry to remove NO_x present in the flue gas are the well stablished SCR (selective catalytic reduction) and SNCR (selective non-catalytic reduction) of NO_x [7, 8]. However, these methods are not able to remove NO_x completely because of some disadvantages during their use at high operating temperatures [9], which also means high costs of the process. The catalysts typically used in SCR, mainly based on V_2O_5, work at temperatures above 300 ºC [10], taking advantage of the high temperatures of the power plants systems but placed in high dust position, promoting catalyst deactivation. However, other industrial units like waste incineration plants and ships demand also low temperature –end-of-pipe- de-NO_x technologies. Therefore, research efforts have been centered on the development of new catalysts able to eliminate NO at lower temperatures. In this sense, not only the reduction process was taken into account, but others such as catalytic oxidation that was proved to work at lower temperature.

Several works were published in this field using zeolites [11] or carbonaceous materials [12] in presence of water at low temperature, giving as conclusion that the reaction occurs in the micropores of the material. Recently, an interesting work published by Ghafari *et al.* reports conversions up to 35 % of NO to NO_2 in presence of water by using a polymer based catalyst at near room temperatures [13]. However, the presence of water decreased the polymer based catalysts performance. For this reason, it is important to develop catalysts are less affected in presence of water, or even with water as promoter to convert NO to value-added products.

Other alternatives to remove NO were also investigated, such as absorption [14, 15]. In this case, the absorption capacity of NO in aqueous solutions is reported to be low [15]. For these reasons, big efforts has been tried to enhancing this absorption capacity by means

of using additives [16]. Furthermore, it was detected the easy combination of NO with transition metals, so different metals were specifically designed for NO capture [17]. All these absorbents were aqueous solutions, limited by the low NO solubility in water [18].

In last years, ionic liquids (ILs) are proposed as new chemical solvents, attracting a huge number of studies in e.g. gas capture applications [19], due to their characteristic properties such as high absorption capacity, low vapor pressure and high thermal and chemical stability [20], among others. Therefore, ILs have been extensively evaluated in gas capture, for instance of CO_2 [21], SO_2 [22], H_2S [23], NH_3 [24], and volatile organic compounds [25]. It is remarkable that, however, few works on NO capture by ILs have been reported so far. Chen *et al.* [26] reported the first functional IL to capture NO, with the disadvantage of the high difficulty in the synthesis stage. Then, Sun *et al.* [27] synthetized a metallic functional ionic liquid able to chemically absorb NO. Recently, Kunov-Kruse *et al.* [28] reported that the IL 1-butyl-3-methylimidazolium nitrate ([bmim][NO_3]) is a successful catalyst for NO oxidation into nitric acid in presence of water. However, it is well stated that the practical application of ILs are limited by their unfavorable transport properties [29, 30]. In fact, several efforts have been centered on developing systems and materials able to reduce the kinetic control in the absorption operations based on ILs [31-33]. Thus, Supported Ionic Liquid Phase (SILP) concept was invented [34-36]. It consists of IL deposition in the pores of a solid support (silica, carbon, among others). In the case of gas capture application, these materials increase the mass transport rates compared with pure ILs due to the increase in the gas-liquid interfaces [37]. In the case of catalysis, it can be used like a solid heterogeneous catalyst for continuous fixed bed reactor systems [35, 38]. Recently, SILPs have been applied to different catalytic reactions. An efficient catalytic system based on metal ligand free in an environmental friendly IL system was successfully developed for Suzuki cross-coupling reactions [39]. Another metal/IL supported on nano-silica based catalysts were employed in the aldehyde C-H activation showing excellent yields of the desired aryl ketones [40]. Catalysts based on copper-doped silica supporting acidic ILs (based on $[HSO_4]^-$ anion) demonstrated a good performance on Biginelly reaction [41]. In last years, CO_2 valorization has attracted the attention of the scientific community, using SILPs as catalysts for the reaction of cycloaddition of epoxides [42, 43]. Regarding NO separation, the first approach using SILP materials (silica as support) was successfully applied by Fehrmann's group [33]. However, the IL loading can limit the practical application of gas capture [32]. A more recent alternative has

emerged: the Encapsulated Ionic Liquids (ENILs) concept, in which a high amount of IL (up to 80%) is contained inside hollow carbon capsules (internal diameter of 400-700 nm) with high specific surface area [31]. The performance of ENIL materials was tested by different gas capture applications such as ammonia [31, 44] and CO_2 in both physical [30, 45] and chemical [46-48] absorption. These works concluded that the encapsulation of the IL does not decrease absorption capacities and increase very significantly the absorption rates, due to the strong increase of contact surface after IL encapsulation. Furthermore, the nature of the IL does not significantly matter to the gas capture kinetics when using ENIL materials, since it is controlled by carbon capsule morphology [48]. Therefore, ENIL materials are able to solve the kinetic restrictions that pure ILs present in gas capture applications.

At this point, it emerged the idea of taking advantage of the improved mass transfer kinetics of ENIL materials for its application in NO oxidation by ionic liquid catalysis. Therefore, we propose 1-butyl-3-methylimidazolium nitrate ([bmim][NO_3]) for its encapsulation into ENIL materials with different loadings. The IL selection was decided based on the previous work in which it was demonstrated that could be NO oxidized. The aim of this work is to evaluate the performance of a new support (based on hollow carbon capsules) in which the IL is encapsulated forming the ENIL materials in NO catalytic oxidation into NO_2, HNO_2 and HNO_3 in presence of water at low temperatures.

Experimental section

Materials

The IL 1-butyl-3-methylimidazolium nitrate (98 %) was purchased from Iolitec. The reagents used for hollow carbon capsules synthesis: phenol (99 %), paraformaldehyde (95-100 %), aluminum trichloride (95-100 %), ammonia (34 %) and absolute ethanol were supplied by Panreac. In addition, tetraethylorthosilicate (98 %) (TEOS), hexadecyltrimethoxysilane (90 %) (C16TMS) and hydrofluoric acid (48 %) were supplied by Sigma-Aldrich. Nitrogen, air and the mixture containing 10,000 ppmv of NO in nitrogen were supplied by AGA. The methanol (99.8 %) used for the promoted NO oxidation was supplied by Sigma-Aldrich.

ENIL synthesis

The hollow carbon capsules (C_{Cap}) were synthetized as ENIL materials following the procedure reported by Büchel *et al.* [49]. This methodology has been successfully

applied by our group in the last years [46, 48, 50, 51] to obtain the C_{Cap} and then the ENIL materials for their use in gas capture applications. The full description of the procedure can be found in the referred works. In summary, C_{Cap} were synthetized following a "templating" method in which the solid core and the mesoporous shell aluminosilicate (SCMS) were used as template. The colloidal solution was maintained at 30 ºC with vigorous stirring to achieve homogenous diameters of the spheres. Then, the shell was grown around the silica core by adding TEOS and C16TMS (to give porosity to the double shell). After being filtrated and calcined at 550 ºC, the SCMS was impregnated by a phenolic resin (generated in situ) that will serve as carbon precursor (prior pyrolysis stage). To accomplish this, aluminum trichloride was impregnated in the SCMS as catalyst of the phenolic resin generation. Then, a mixture of paraformaldehyde and phenol was added to completely impregnate the material generating the phenol-paraformaldehyde resin. The resulting material could be heated until 160 ºC that is the curing temperature of the resin, during 5 hours and then increased until 850 ºC under a nitrogen atmosphere to accomplish the pyrolysis of the material. The resulting carbon was washed with HF in order to remove the remaining silica present, being able to obtain the final hollow carbon capsules (C_{Cap}).

From C_{Cap}, the ENIL materials were prepared using incipient wetness impregnation. 400 mg of C_{Cap} were used and 1 mL of methanol-IL solution was added drop by drop onto the carbon support. Then, the resulting ENIL materials were heated until 85 ºC to completely remove the remaining methanol. In this work, four different ILs loadings were tested (20, 40, 60, and 80 % w/w). The complete synthesis process is shown in Scheme 1. The methodology used was applied in several works of our group demonstrating the homogenous distribution of the IL inside the C_{Cap} [30, 44, 46-48].

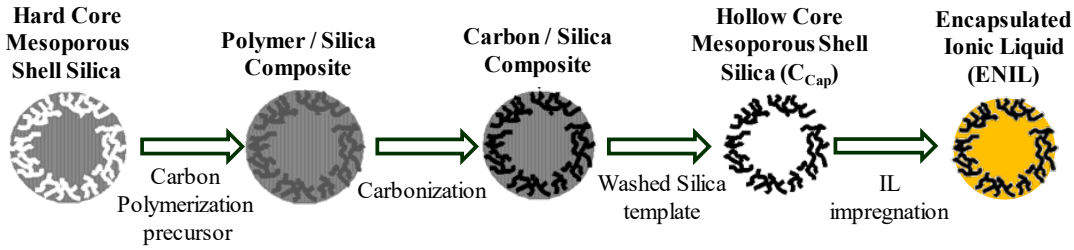

Scheme 1: ENIL synthesis scheme

ENIL characterization

The C_{Cap} samples were characterized by means of elemental analysis in a LECO CHNS-932 apparatus. The porous structure of the hollow spheres and ENIL materials

was also characterized by 77 K N_2 adsorption/desorption using a TriStar II 3020 (Micromeritics) equipment after 10 h of degassing at 0.1 mbar and 393 K. The pore size distribution was calculated using t method. The microstructure and morphology of C_{Cap} were studied by transmission electron microscopy (TEM) using a JEOL JEM 2100 HT microscope. Then, the ENIL materials prepared were characterized by means of thermal gravimetric analysis (TGA) and elemental composition to check the amount of IL inside the material before and after reaction using a Mettler Toledo TGA/DSC 1 STARe system. This was carried out under a N_2 flow of 50 mL/min from room temperature until 600 ºC with a heating rate of 10 ºC/min.

NO oxidation measurements

The prepared ENIL materials and hollow carbon spheres (C_{Cap}) were tested as NO catalysts using a fixed-bed reactor with ENILs volume of approximately 1.2 cm^3, corresponding to masses between 0.4-1.0 g depending on the load of IL used. Most experiments were carried out at room temperature (near 24 ºC). However, in the experiments in which the temperature was changed, the reactor was placed inside an oven able to control the temperature (regeneration experiments as well). A flue gas was passed through the reactor with a NO concentration of 2,000 ppm. The O_2 content was varied from 6.2 to 16.8 % and balanced with N_2. Three mass flow controllers were used: i) connected to a 1% NO-N_2 bottle; ii) connected to an air bottle; iii) connected to a N_2 bottle. The total gas flow for each experiment was set at 200 mL/min. All the reactions were conducted at atmospheric pressure. Furthermore, the top of the reactor was fitted with a three-way valve that allows introducing the gases and the liquid inside the fixed-bed reactor. The flow of the liquid was controlled by a NE-300 Syringe Pump. In this sense, the relative humidity (RH) of the flue gas was changed and studied from 10 to 75 % utilizing a syringe filled of deionized water. The addition of the methanol to promote the oxidation reaction was accomplished by adding a water/methanol solution to the system by the Syringe Pump. The methanol concentration (varied from 100 to 1600 ppm) and the flow rate needed were calculated in each experiment in order to maintain the desired conditions. The bottom of the reactor was conducted into a gas cuvette inside a Thermo Scientific Evolution 220 UV-Visible Spectrophotometer. Each measurement collects the whole spectrum from 200 to 600 nm. NO have absorption bands in the ultra-violet (UV) region at 204 nm, 215 nm and 226 nm. This last peak was used to quantify the NO in the exit of the reactor and calculate the conversion. Peakfit.m matlab script was

used for deconvolution of the three peaks, using last one at 226 nm to calculate conversions as a function of the peak area using a standard curve performed with different NO concentrations mixed with an inert gas (N_2). Other peaks that could be identified in the spectra are due to NO_2 having a broad peak around 405 nm and HNO_2 that presents four different peaks from 340 to 390 nm; and the HNO_3 exhibiting a broad peak in the NO region (from 200 to 250 nm). These peaks can indicate which species are being formed depending on the operation conditions tested. In all cases, the conversion was calculated at steady state, i.e. identical spectra obtained during at least 2 hours. Before changing the relative humidity of the inlet gas, the desorption experiment was carried out after heating the sample up to 130 ºC using 100 mL/min of N_2 in presence of water (ratio 1:1) to totally remove the water, methanol and nitric acid present in the sample.

Results

C_{Cap} and ENILs characterization

The hollow carbon capsules (C_{Ccap}) and the four prepared ENIL materials were characterized by means of microscopy, pore structure, elemental analysis and thermal stability. Thus, Figure 1A shows TEM microscopy image of the C_{cap} while Figure 1C shows the size distribution of the analyzed sample by several TEM images. Figure 1B presents the N_2 adsorption-desorption isotherm of the C_{Ccap} before the incorporation of [bmim][NO_3] IL.

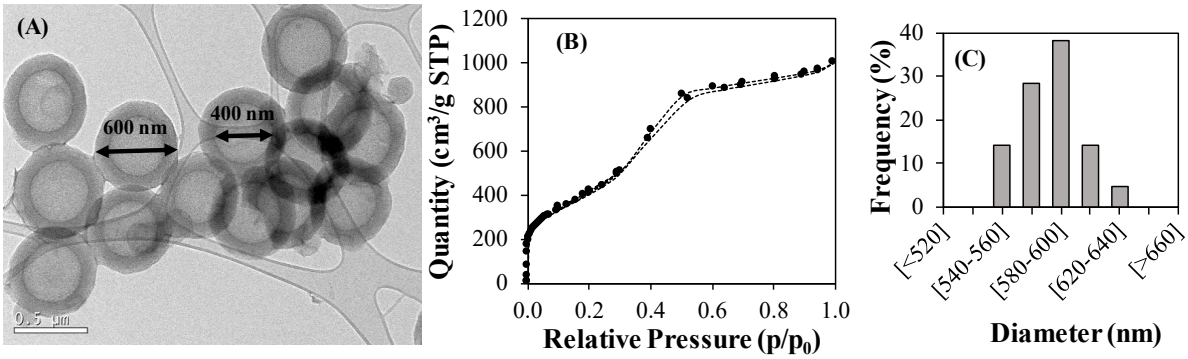

Figure 1: **(A)** TEM image of the hollow carbon capsules (C_{Ccap}) to prepare ENIL materials; **(B)** N_2 adsorption/desorption isotherms @ 77 K of C_{Ccap} and **(C)** size distribution of C_{Ccap}

Figure 1A shows the homogenous size distribution of the material with spherical shape and an external diameter of almost 600 nm with a shell thickness of 200 nm and a large central hole. The N_2 adsorption-desorption isotherm (Figure 1B) is typical of a mesoporous material with a significant microporosity contribution (both as a consequence

214 of the porosity of the shell). Table 1 reflects the elemental analysis and the summarized
215 information extracted from the N_2 adsorption-desorption isotherms.

216

217 Table 1: Carbon capsules (C_{Cap}) characterization by means of elemental analysis and N_2
218 adsorption-desorption @ 77 K.

Characterization technique			
Elemental Analysis		N_2 adsorption-desorption	
% C (w)	91.40	S_{BET} (m^2/g)	1,494
% H (w)	1.80	$V_{micropore}$ (cm^3/g)	0.55
% N (w)	0.10	$V_{mesopore}$ (cm^3/g)	0.68
		Pore size (Å)	41.35

219

220 The elemental analysis extracted from Table 1 confirm the carbonaceous nature of
221 the material (more than 90% of carbon). The incorporation of the different amounts of IL
222 in the support is possible due to the high porosity. The material possesses both
223 mesoporosity and microporosity mainly based on the porous shell grown around the
224 central hollow core. Thus, the average pore size is almost 40 Å, which reflects the
225 mesoporosity of the material. In that way, the different amounts of IL can be incorporated
226 in the support filling the double shell first (until 40% of IL) and the large central hole
227 afterwards [31]. Once the C_{Cap} was synthetized and characterized, the ENIL materials can
228 be prepared with different amounts of IL. In order to check the amount of IL incorporated
229 in each sample, Figure 2 shows the TGA analysis of each one.

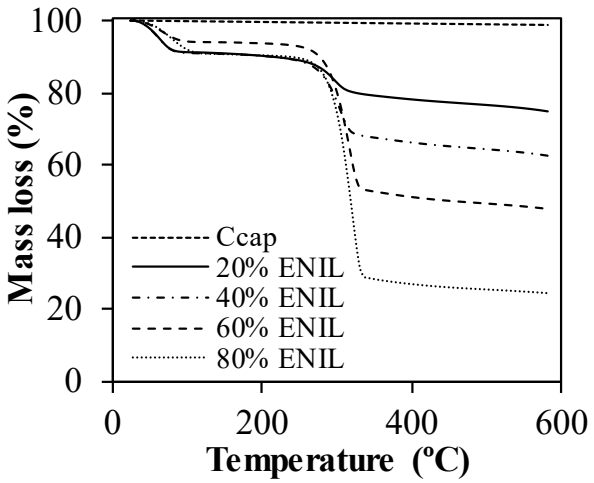

230 Figure 2: TGA analysis of the materials used in this work: hollow carbon capsules (C_{cap})
231 and ENIL materials with four different IL loading (20, 40, 60 and 80 % of [bmim][NO_3]).
232 Analysis carried out with a temperature increase of 10 ºC·min^{-1} under 50 mL·min^{-1} of N_2.

Starting with the TGA analysis of C_{Cap}, as can be seen in Figure *2*, our support is stable at least until 600 ºC under nitrogen. Therefore, using this curve as reference, it is possible to estimate the amount of IL present in each sample taking into account the remaining mass at 600 ºC (attributed to the carbon support). In all cases, after a little decay prior to 100 ºC (possible sorbed water) the final value corresponds perfectly to the nominal amount of each material. The elemental composition results of each material (see Table S1 of Supplementary Information) confirm the conclusions of TGA analysis. In addition, the pore size distribution of all the ENIL materials are shown on Figure S1 of the Supplementary Information confirming almost the same average pore size (40 Å) but decreasing the pore volume by increasing the IL load on ENILs. The experimental N_2 adsorption/desorption isotherms are also included in Figure S2 of Supplementary Information. An increase in the IL loading inside ENIL material leads to the filling of the pores until 60-80%, in which all remained completely occupied or blocked by IL [31, 32].

NO oxidation in dry conditions

The different prepared catalysts were first tested in absence of moisture. Prior to test the ENIL materials performance in NO catalytic oxidation, it is important to understand the behavior of the support (C_{Cap}) under different oxidation conditions. Figure 3 shows the NO conversion in the hollow carbon capsules using different O_2 contents. In this case, the reaction involved in experiments in dry oxygen condition is depicted in Eq. 1.

$$NO + ½\ O_2 \rightarrow NO_2 \qquad (1)$$

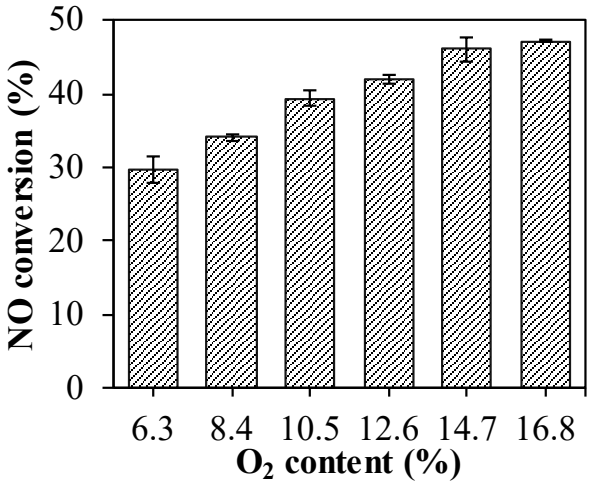

Figure 3: NO conversion of hollow carbon capsules (C_{cap}) in dry conditions at different oxygen contents. Gas composition: 2,000 ppm NO, 6.3-16.8% O_2, balance N_2, Flow: 200 mL·min^{-1}, GHSV=10,000 h^{-1}. Experiments conducted at room temperature.

As can be seen, the trend clearly shows higher catalytic activity by increasing the amount of O_2 in the system, reaching almost 48 % of conversion at 16.8% of O_2. This means that the presence of more O_2 in the system leads to the formation of more NO_2, resulting in higher conversion values (see Figure S3 in Supporting Information). Compared to those previously reported in the literature, we used 10.5% O_2 (almost 40 % NO conversion) which corresponds to those applied at industrial conditions to treat almost 2,000 ppm of NO [52]. Zeolite based catalysts exhibit NO conversions from 5 to 45 % [11] depending on the modifications carried out, concluding that those with higher micropore volume show the greatest performance. Zhang *et al.* [12] reported NO conversions up to 57 % using microporous activated carbons. Sousa *et al.* [53] used doped carbons reaching conversions up to 75 % in the best case. In view of all these results, our C_{Cap} material, later used as support for ENIL materials, presents NO conversion in dry O_2 conditions in the range of the zeolite catalysts and slightly lower when compared with activated carbons prior to their modification at almost same conditions. These differences may be attributed to the different porous structure of the materials. It is believed and proved that a high microporous structure leads to higher conversions. In the case of our material, it is basically a mesoporous material but presenting high micropore volume (see Table 1). The C_{Cap} performance can be compared with the ENIL catalysts at 10.5% of O_2. In Figure 4,

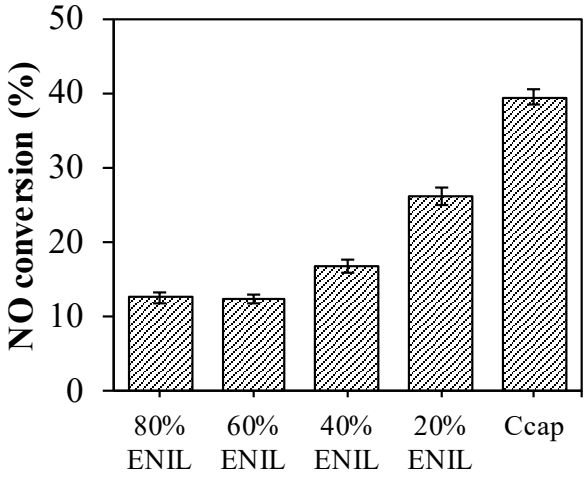

the NO conversion reached by each material (including the previous discussed C_{Cap}) are compared.

Figure 4: NO conversion of the different materials of the work in dry conditions. Gas composition: 2,000 ppm NO, 10.5% O_2, balance N_2, Flow: 200 mL·min^{-1}, GHSV=10,000 h^{-1}. Experiments conducted at room temperature.

As can be seen, NO conversion decreases by increasing the amount of IL in the catalyst until the conversion remains constant (from 60% IL loading). This could be

explained due to filling of the pores of the C_{Cap} material (see the reduction in BET area while increasing the IL loading in Table S1 of the Supplementary Information). In the case of 20% and 40% ENIL material, the higher conversion may be attributed to partly filled pores exhibiting more efficient IL distribution on the pore surface. From the previous reported data with [bmim][NO_3] IL [28], it seems that the presence of water is key leading to the formation of more $[NO_3]^-$ anions (anion part of the IL) that may improve the NO removal.

NO oxidation in wet gas

In order to simulate near industrial conditions the catalytic performance of our materials was investigated in gas streams that contain around 10% O_2 and water. Experiments in wet conditions follow the reaction of Eq. 2. More details about the mechanism of NO oxidation reaction in presence of water using [bmim][NO_3] can be found in previous works [28, 54].

$$4\ NO + 3\ O_2 + 2\ H_2O \rightarrow 4\ HNO_3 \qquad (2)$$

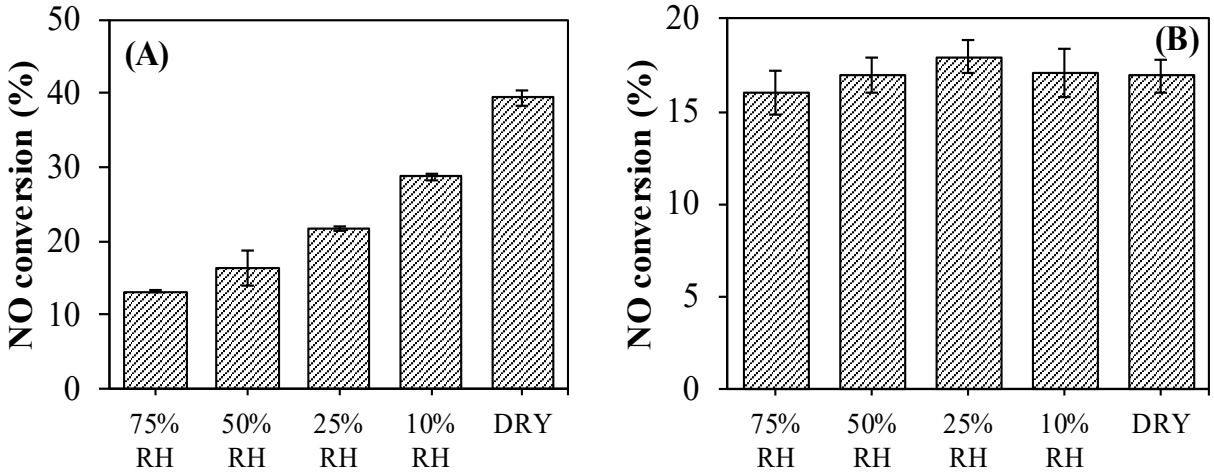

Figure 5: NO conversion of **(A)** the hollow carbon capsules (C_{cap}) and **(B)** the 40 % [bmim][NO_3] ENIL material in different dry and wet conditions (from 10 to 75% Relative Humidity). Gas composition: 2,000 ppm NO, 10.5% O_2, balance N_2, Flow: 200 mL·min^{-1}, GHSV=10,000 h^{-1}. Experiments conducted at room temperature.

Figure 5A clearly shows the catalytic inhibition when water was added into the system employing C_{Cap} as catalyst. NO conversion reaches only a value of 13% at 75% RH. This may be explained by the decrease of the NO adsorption mainly caused by the competitive water adsorption. Some works reported that water affects negatively the NO oxidation using activated carbons (AC) or zeolites. They reached the same conclusion: the NO oxidation inhibition in presence of water is caused by adsorption competition.

Thus, Mochida *et al.* [55] showed a huge decrease in conversion by increasing RH in AC catalysts. Another work by Mochida *et al.* [56] showed the limitation of RH > 60% to the NO oxidation using AC catalysts. Guo *et al.* [57] reported the complete stop in NO oxidation when RH is higher than 20% using AC catalysts. The moisture influence was also studied in zeolite based catalysts [58] reaching conversions of only 10% when 8% of H_2O is present in the flue gas stream, showing a dramatic inhibiting effect in that kind of catalysts. The most recent study at wet conditions concerns a new polymer based catalyst [13] in which the inhibition was also demonstrated when 50% RH was employed. In addition, we believe that the inhibition may also be caused by means of *capillary condensation*, described by the Kelvin equation [59]. At the pore diameter of C_{Cap} (about 41 Å, see Table 1), *capillary condensation* at room temperature is expected to occur at a RH around 50-60% [60] and may thus cause the observed deactivation in Figure 5A for RH > 50%. This phenomenon definitely does not occur when the IL is completely filling the pores of the support. As can be seen, the presence of water does not inhibit the NO oxidation when using ENIL material. This may be explained by the different NO oxidation mechanism by the [bmim][NO_3] catalyst in presence of water that leads to conversion to HNO_3 instead of NO_2 in the dry gas as concluded in the previous work [28]. A slight increase in the HNO_3 and decrease in the NO_2 regions of the UV-Vis spectrum (see Figure S2 in Supporting Information) was thus found by adding water to the system compared to the C_{Cap} catalyst. Therefore, this IL catalyst the first reported NO oxidation catalyst that is not negatively affected by presence of water.

Figure 6 shows the NO conversion of the studied materials at two different gas humidity levels.

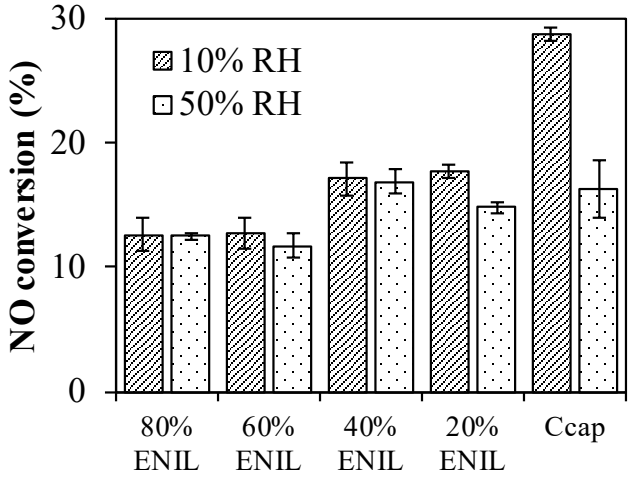

Figure 6: NO conversion of the different materials at two different wet conditions (10 and 50% Relative Humidity). Gas composition: 2,000 ppm NO, 10.5% O_2, balance N_2, Flow: 200 mL·min^{-1}, GHSV=10,000 h^{-1}. Experiments conducted at room temperature.

For 10% RH, it can be seen that the C_{Cap} material exhibits the highest conversion compared to the ENILs. It seems therefore the water levels are not enough for the ENIL materials to exhibit a decreased performance. The conversion follows almost the same trend as observed for the dry experiments, i.e. the NO conversion decreases while increasing the amount of IL in the material until 60% loading above, which it remains constant. However, a closer look reveals that the presence of water in the gas for the 20% ENIL catalyst seems to be partially inhibited compared to dry conditions, as in the case for the C_{Cap}. This may mean that there are still some pores not completely filled with the IL.

Analyzing the 50% RH exposure, the presence of available pores for NO oxidation in the case of 20% ENIL material seems obvious due to the observed reduction in the NO conversion (but to a lesser extent than for C_{Cap}) when compared with 10% RH exposure. This behavior was also concluded in terms of available pores while increasing the amount of ILs in the support by Lemus *et al.* [31, 32]. The rest of the materials exhibit unaltered behavior, since their activities are not affected by the addition of more water. If we now compare the performance of the materials at 50% RH, it can be seen that the 40% ENIL exhibits slightly higher NO conversion than C_{Cap}, probably due to the difference in mechanism, while the 20% ENIL material shows almost the same behavior as C_{Cap}, followed closely by the other two ENILs. Thus, it can be concluded that flue gas streams that contain high amount of water does not affect the ENIL materials performance (in terms of NO conversion), in contrast to the typical carbon materials (C_{Cap}), in which the reaction is strongly inhibited.

Methanol promoted NO oxidation in wet gas

In the 1990's, methanol promoted NO oxidation at high temperatures (from 700 ºC up to 1,000 ºC) was investigated [61, 62]. An increase in terms of NO conversion was reported when methanol was added to the system. Zamansky *et al.* proposed [62] the addition of a MeOH/H_2O_2 mixture to further increase the catalytic performance. No more work related to the methanol promoted NO oxidation has been published as far as we know. Then, research efforts moved to methanol oxidation in presence of NO. Thus, some papers [63-65] showed an increase in the MeOH conversion in presence of NO (temperatures

from 600 up to 1,200 ºC). Furthermore, they proposed a possible mechanism of the oxidation reaction, concluding that radical formation in presence of NO was occurring. Since methanol promotes the NO oxidation, we screened different methanol concentrations to examine our catalysts performance. As far as we know, this is the first work in which this methodology is applied at room temperature using IL-based catalysts. Thus, Figure 7 shows the NO conversion as a function of the RH and the methanol concentration for the 40% ENIL material.

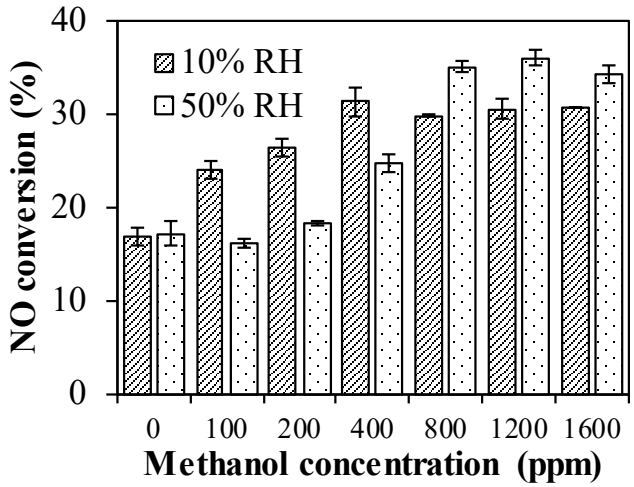

Figure 7: NO conversion in 40% [bmim][NO_3] ENIL material with relative humidity of 10 and 50% and different concentrations of MeOH in the gas phase. Gas composition: 2,000 ppm NO, 10.5% O_2, balance N_2, Flow: 200 mL·min^{-1}, GHSV=10,000 h^{-1}. Experiments conducted at room temperature.

From Figure 7, it can be seen how the NO conversion increases by increasing the methanol concentration until reaching a maximum. That maximum depends on the RH studied but it is located at a MeOH/NO ratio between 0.2-0.4 depending on the RH. Starting with 10% RH, it is clearly seen that NO conversion increases while increasing the amount of methanol until 400 ppm of MeOH whereafter it remains constant up to 1,600 ppm of MeOH. For 50% RH, the same trend is observed but the maximum is reached at 800 ppm of MeOH. It seems that for 50% RH, the NO conversion is higher than at 10% RH at methanol concentrations above 800 ppm. This interesting difference in the trends might be explained by increased HNO_3 formation when more water is present in the system (see figure S4 of the Supporting Information). An interesting work by Xiao *et al.* [66] studying the mechanism of the methanol oxidation in presence of NO (room temperature performed as well) indicated that NO_2 may play a role in the methanol oxidation. They proposed a series of intermediate reactions involved in the MeOH

oxidation when NO_2 is present. In this context, we believe that two of the proposed reactions may be occurring in our system:

$$CH_3OH + \cdot NO_2 \rightarrow \cdot CH_2OH + HONO \quad (3)$$

$$CH_3OH + \cdot NO_2 \rightarrow CH_3O\cdot + HONO \quad (4)$$

Reactions (3) and (4) may be occurring in our system due to the observed nitrous acid (HONO) and the absence of NO_2 in the UV-Vis spectrum (see Figure S5 in Supporting Information), not only while adding the first droplets but also at the steady state (especially when high conversions were found). This was immediately found when methanol was added to the system. Furthermore, huge amounts of HNO_3 were detected while adding MeOH to the system (see Figure S5 in Supporting Information), this may be explained by the proposed mechanism by Kunov-Kruse *et al.* [28] when using [bmim][NO_3] as catalyst in which HNO_3 was formed in the catalytic reaction in presence of water. In addition, the presence of HONO may lead to fast formation of HNO_3 (due to nitrous acids well-known instability). Therefore, promoted oxidation of NO in presence of MeOH may be explained by radical formation in both the liquid and the gas phase. Low amounts of MeOH that remain absorbed on the IL are simply removed by heating up the sample to 130 ºC. This compound can be easily separated from the others involved in the reaction due to the high differences in their volatilities. Future works will be centered on the study of the mechanism of reaction, getting attention the possible other value-added products formed during the reaction.

Based on the optimized MeOH addition, two different concentrations for each RH (200 and 400 ppm for 10% RH and 400 and 800 ppm for 50% RH) respectively were selected for testing the different materials.

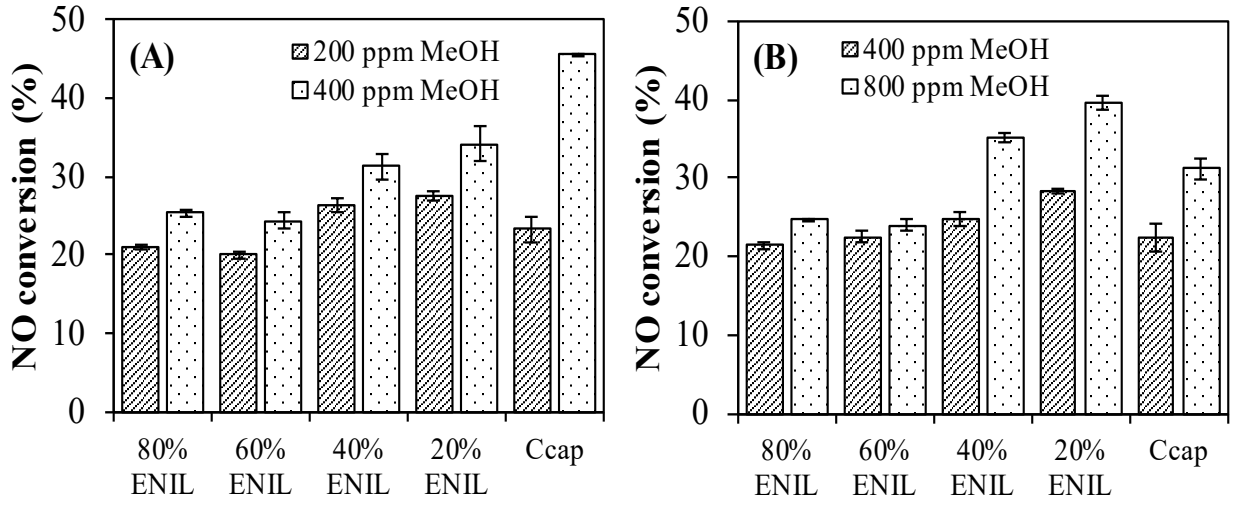

Figure 8: NO conversion of the different materials at relative humidity of **(A)** 10% RH and **(B)** 50% RH and two different concentrations of MeOH in the gas phase. Gas composition: 2,000 ppm NO, 10.5% O_2, balance N_2, Flow: 200 mL·min^{-1}, GHSV=10,000 h^{-1}. Experiments conducted at room temperature.

In Figure 8A, the methanol promoted NO conversions of the different materials at 10% RH can be analyzed. In general terms, all the materials exhibit greater conversions with the addition of MeOH when compared to the same moisture conditions without MeOH. For 200 ppm methanol, it can be seen that the 20% ENIL material presents the highest NO conversions while it seems that the amount of MeOH added is not enough for overcoming the inhibition in C_{Cap} material pores. However, when increasing to 400 ppm of MeOH, the hollow carbon capsules exhibit the highest activity. The measurements show in general that the addition of methanol promotes the reaction at wet conditions independent of the catalyst used.

Figure 8B shows that the 20% and 40% ENIL materials present the highest conversion at 50% RH, even higher than hollow carbon capsules. This suggests that at high concentrations of water, the presence of MeOH is not compensating for the inhibition of the NO reaction in the C_{Cap} material probably due to pore condensation of water. The results confirm that for wet conditions with addition of methanol, the ENIL materials exhibit a positive effect regarding the NO removal (increase of more than 50% in NO conversion when compared to the same moisture conditions without methanol - Figure 6).

It is important to remark that after testing the performance of each material, TGA analysis was performed to check the amount of IL that remains in the support (see Figure S6 in Supporting Information) after adding water and methanol to the system. In all cases,

435 it was obtained that the same initial amount of IL remained inside the support compared
436 to before the catalytic tests.

437 Table 2: NO oxidation performance of different catalysts for dry and wet conditions

Catalyst	NO dry conversion (%)	NO wet conversion (%)	Ref.
Active carbon	69	0	[57]
Active carbon	94	0	[57]
Active carbon nanofibers	73	18	[55]
Active carbon nanofibers	64	16	[55]
Active carbon fibers	89	15	[56]
Porous polymers	43	35	[13]
Porous polymers	48	31	[13]

438

439 Table 2 summarizes NO conversion results previously reported in the literature in
440 dry and wet conditions. The experimental conditions are close to those used in our work.
441 As shown, catalysts based on active carbon present a practically complete inhibition when
442 water is added to the system. On the contrary, catalysts based on porous polymers were
443 reported as first materials able to oxidize NO in wet conditions, reaching a NO conversion
444 of 35%. The difference between ENIL materials and those previously reported is that they
445 are not inhibited when water is present in the system, obtaining almost the same NO
446 conversion independently of the amount of water. In fact, 40% NO conversion is the
447 maximum reached for 20% ENIL catalysts in wet conditions. Therefore, it can be
448 concluded that ENIL materials may be an alternative for catalysts typically studied on the
449 literature.

450 *Temperature effect on NO conversion*

451 Previous studies reported an increased NO conversion when decreasing the
452 temperature (a negative apparent activation energy) [67, 68], in good agreement with
453 homogenous phase oxidation [67]. Figure 9 shows the NO conversion as a function of the
454 temperature for the C_{Cap} material and the ENIL materials at 50% RH and 800 ppm of
455 MeOH.

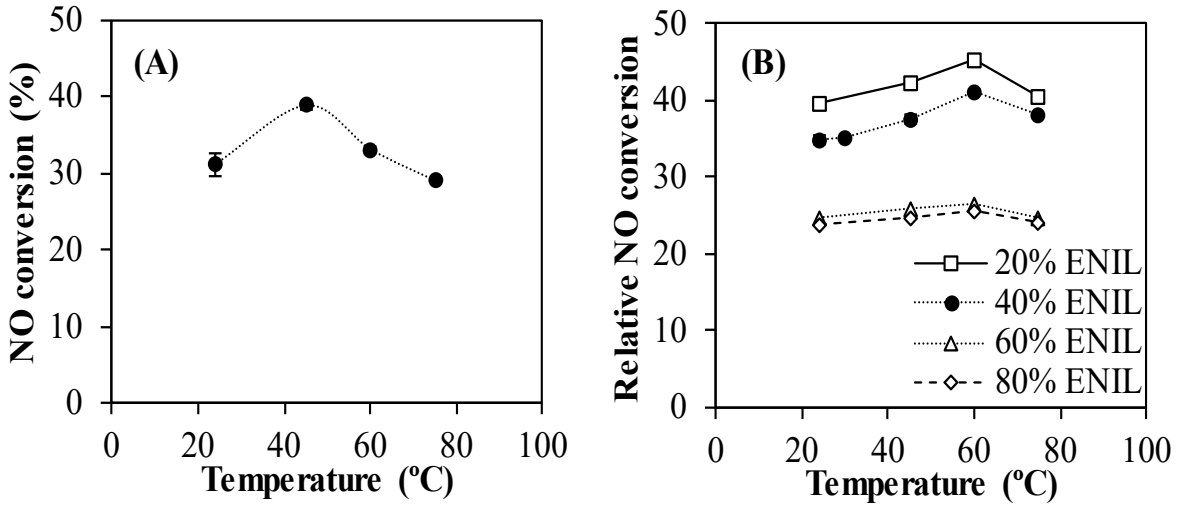

Figure 9: NO conversions in **(A)** hollow carbon capsules (C_{cap}) and **(B)** ENIL materials as a function of the temperature using 50% Relative Humidity and 800 ppm of MeOH in the gas phase. Gas composition: 2,000 ppm NO, 10.5% O_2, balance N_2, Flow: 200 $mL \cdot min^{-1}$, GHSV=10,000 h^{-1}.

As shown in Figure 9A, the C_{Cap} material optimum was found at 45 ºC while in the case of the ENIL material (Figure 9B), the maximum is located at 60 ºC. In the case of the ENIL material, the maximum at 60 ºC may be attributed to the competing limitations (radical formation) at low temperature and the lower gas solubility in the IL at higher temperatures. These conclusions concern the 20 and 40% ENIL materials in which most of the IL seems to be accessible to the gas, contrary to the 60 and 80% ENILs, where the temperature does not affect the NO conversion. The different temperature effect observed on C_{Cap} and ENIL materials may be caused by the place in which the reaction is occurring, i.e pores of C_{Cap} and IL of ENIL materials. Moreover, it may be easier to retain the absorbed gas on the liquid media than on pores of solid material when temperature is increased. However, in general, the impact of the temperature on the NO conversion is not very important, reaching about 25% at maximum.

It can be concluded that the oxidation at higher temperatures (approaching flue gas stack temperatures) results in a slight increment of NO conversion, i.e. at temperatures close to 60 ºC, the NO conversion is in the range of 45%, in presence of water in the gas phase.

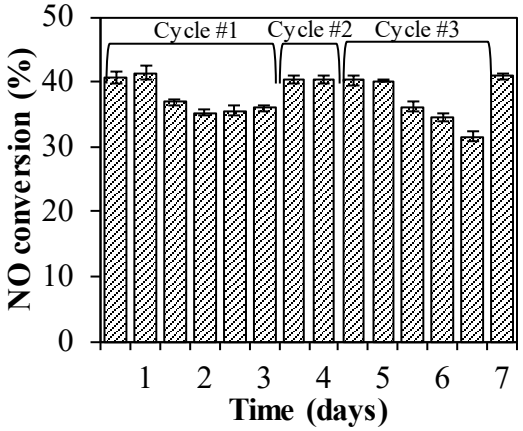

Figure 10: Stability measurements using 20% ENIL material using 50% Relative Humidity and 800 ppm of MeOH in the gas phase. Gas composition: 2,000 ppm NO, 10.5% O_2, balance N_2, Flow: 200 mL·min^{-1}, GHSV=10,000 h^{-1}.

Figure 10 presents the stability measurements of 20% ENIL material in four different cycles. As can be seen, NO conversion is maintained for 24 hours. Then, it started to decrease due to the IL saturation by NOx and HNO_3 formed. The increase in the temperature up to 130 ºC allows the complete regeneration of the catalyst reaching the same values of the fresh one. Therefore, it was demonstrated one day stability and the easy regeneration of the catalyst by a simple temperature increase.

Encapsulated Ionic Liquids (ENILs) were successfully applied as catalysts for NO oxidation at low temperatures. ENILs with different loads of the IL [bmim][NO_3] were synthetized and then characterized by means of elemental analysis, thermal stability, porous structure and microscopy. Experiments in dry gas show higher NO conversion of the hollow carbon capsules compared to ENILs, where the conversion increased with decreasing the IL loading. Experiments conducted at different relative humidities showed positive effect on NO conversion for the ENIL materials. On the contrary, the results of empty carbon material showed inhibition of the NO oxidation by increasing humidity in the system. The reaction was promoted (in presence of water) by addition of methanol to the system. The amount of methanol added to the system was optimized (at different RH), showing an optimal MeOH/NO ratio between 0.2-0.4. In this case, ENILs composed of 20 and 40% of IL exhibited the greatest performance (including hollow carbon capsules) reaching conversions near 45%. The temperature effect on the reaction revealed an optimum temperature of 60 ºC when using ENILs, accomplishing relative NO conversions 20% higher than at room temperature ones. Stability measurements revealed

NO conversion is maintained during at least 24 h without any loss. The catalyst was easily regenerated by increasing the temperature up to 130 ºC. These results demonstrate potential application of ENILs as catalysts at near industrial flue gas conditions to create "fast SCR" for a down-stream traditional SCR catalyst.

Supporting Information: Elemental composition characterization of ENIL materials involved in the work. Pore size distribution of the materials involved in the work. N_2 adsorption/desorption isotherms @ 77 K of all the materials involved in the work. UV-Vis Spectrum of hollow carbon capsules (C_{Cap}) in dry conditions at different oxygen contents. UV-Vis Spectrum of 40% [bmim][NO_3] ENIL material (40% ENIL) in dry and 10% Relative Humidity conditions. UV-Vis Spectrum of 20% [bmim][NO_3] ENIL material (20% ENIL) in 50% Relative Humidity and 800 ppm of MeOH conditions. TGA analysis of the materials used in this work: hollow carbon capsules (C_{Cap}) and ENIL materials with four different IL loads (20, 40, 60 and 80 % of [bmim][NO_3]) after being used in the catalytic reactions.

Acknowledgments

The authors thank the Ministerio de Economía y Competitividad (MINECO) of Spain (project CTQ2017-89441-R) and Comunidad de Madrid (P2018/EMT4348) for financial support. Rubén Santiago also thanks David Nielsen for his great support at DTU.

References

1. Chang, S. G.; Liu, D. K., Removal of nitrogen and sulphur oxides from waste gas using a phosphorus/alkali emulsion. *Nature* **1990,** *343*, 151.
2. Pham, E. K.; Chang, S.-G., Removal of NO from flue gases by absorption to an iron(ii) thiochelate complex and subsequent reduction to ammonia. *Nature* **1994,** *369*, 139.
3. Kanchongkittiphon, W.; Mendell, M. J.; Gaffin, J. M.; Wang, G.; Phipatanakul, W., Indoor Environmental Exposures and Exacerbation of Asthma: An Update to the 2000 Review by the Institute of Medicine. *Environmental Health Perspectives* **2015,** *123* (1), 6-20.
4. Solomon, S., Stratospheric ozone depletion: A review of concepts and history. *Reviews of Geophysics* **1999,** *37* (3), 275-316.
5. Volz, A.; Kley, D., Evaluation of the Montsouris series of ozone measurements made in the nineteenth century. *Nature* **1988,** *332*, 240.
6. Liu, N.; Lu, B.-H.; Zhang, S.-H.; Jiang, J.-L.; Cai, L.-L.; Li, W.; He, Y., Evaluation of Nitric Oxide Removal from Simulated Flue Gas by Fe(II)EDTA/Fe(II)citrate Mixed Absorbents. *Energy & Fuels* **2012,** *26* (8), 4910-4916.
7. Jirat, J.; Stepanek, F.; Marek, M.; Kubicek, M., Comparison of design and operation strategies for temperature control during selective catalytic reduction of NOx. *Chemical Engineering & Technology* **2001,** *24* (1), 35-40.

8. Maisuls, S. E.; Seshan, K.; Feast, S.; Lercher, J. A., Selective catalytic reduction of NOx to nitrogen over Co-Pt/ZSM-5: Part A. Characterization and kinetic studies. *Applied Catalysis B: Environmental* **2001,** *29* (1), 69-81.
9. Gao, Y.; Luan, T.; LÜ, T.; Cheng, K.; Xu, H., Performance of V2O5-WO3-MoO3/TiO2 Catalyst for Selective Catalytic Reduction of NOx by NH3. *Chinese Journal of Chemical Engineering* **2013,** *21* (1), 1-7.
10. Busca, G.; Lietti, L.; Ramis, G.; Berti, F., Chemical and mechanistic aspects of the selective catalytic reduction of NOx by ammonia over oxide catalysts: A review. *Applied Catalysis B: Environmental* **1998,** *18* (1), 1-36.
11. Zhang, Z.; Atkinson, J. D.; Jiang, B.; Rood, M. J.; Yan, Z., NO oxidation by microporous zeolites: Isolating the impact of pore structure to predict NO conversion. *Applied Catalysis B: Environmental* **2015,** *163*, 573-583.
12. Zhang, Z.; Atkinson, J. D.; Jiang, B.; Rood, M. J.; Yan, Z., Nitric oxide oxidation catalyzed by microporous activated carbon fiber cloth: An updated reaction mechanism. *Applied Catalysis B: Environmental* **2014,** *148-149*, 573-581.
13. Ghafari, M.; Atkinson, J. D., Catalytic NO Oxidation in the Presence of Moisture Using Porous Polymers and Activated Carbon. *Environ Sci Technol* **2016,** *50* (10), 5189-5196.
14. Long, X. L.; Xin, Z. L.; Chen, M. B.; Xiao, W. D.; Yuan, W. K., Nitric oxide absorption into cobalt ethylenediamine solution. *Separation and Purification Technology* **2007,** *55* (2), 226-231.
15. Khan, N. E.; Adewuyi, Y. G., Absorption and Oxidation of Nitric Oxide (NO) by Aqueous Solutions of Sodium Persulfate in a Bubble Column Reactor. *Industrial & Engineering Chemistry Research* **2010,** *49* (18), 8749-8760.
16. Demmink, J. F.; van Gils, I. C. F.; Beenackers, A. A. C. M., Absorption of Nitric Oxide into Aqueous Solutions of Ferrous Chelates Accompanied by Instantaneous Reaction. *Industrial & Engineering Chemistry Research* **1997,** *36* (11), 4914-4927.
17. Chien, T. W.; Hsueh, H. T.; Chu, B. Y.; Chu, H., Absorption kinetics of NO from simulated flue gas using Fe(II)EDTA solutions. *Process Safety and Environmental Protection* **2009,** *87* (5), 300-306.
18. Zhu, H.-S.; Mao, Y.-P.; Chen, Y.; Long, X.-L.; Yuan, W.-K., Removal of nitric oxide and sulfur dioxide from flue gases using a FeII-ethylenediamineteraacetate solution. *Korean Journal of Chemical Engineering* **2013,** *30* (6), 1241-1247.
19. Welton, T., Ionic liquids: a brief history. *Biophys Rev* **2018,** *10*, 691-706.
20. Kosmulski, M.; Gustafsson, J.; Rosenholm, J. B., Thermal stability of low temperature ionic liquids revisited. *Thermochimica Acta* **2004,** *412* (1), 47-53.
21. Aghaie, M.; Rezaei, N.; Zendehboudi, S., A systematic review on CO2 capture with ionic liquids: Current status and future prospects. *Renewable & Sustainable Energy Reviews* **2018,** *96*, 502-525.
22. Lin, H.; Bai, P.; Guo, X. H., Ionic Liquids for SO2 Capture: Development and Progress. *Asian J. Chem.* **2014,** *26* (9), 2501-2506.
23. Wang, L. Y.; Xu, Y. L.; Li, Z. D.; Wei, Y. N.; Wei, J. P., CO2/CH4 and H2S/CO2 Selectivity by Ionic Liquids in Natural Gas Sweetening. *Energy & Fuels* **2018,** *32* (1), 10-23.
24. Bedia, J.; Palomar, J.; Gonzalez-Miquel, M.; Rodriguez, F.; Rodriguez, J. J., Screening ionic liquids as suitable ammonia absorbents on the basis of thermodynamic and kinetic analysis. *Separation and Purification Technology* **2012,** *95*, 188-195.
25. Bedia, J.; Ruiz, E.; de Riva, J.; Ferro, V. R.; Palomar, J.; Jose Rodriguez, J., Optimized Ionic Liquids for Toluene Absorption. *AlChE J.* **2013,** *59* (5), 1648-1656.

26. Chen, K. H.; Shi, G. L.; Zhou, X. Y.; Li, H. R.; Wang, C. M., Highly Efficient Nitric Oxide Capture by Azole-Based Ionic Liquids through Multiple-Site Absorption. *Angewandte Chemie-International Edition* **2016,** *55* (46), 14362-14366.
27. Sun, Y.; Ren, S.; Hou, Y.; Zhang, K.; Wu, W., Absorption of nitric oxide in simulated flue gas by a metallic functional ionic liquid. *Fuel Processing Technology* **2018,** *178*, 7-12.
28. Kunov-Kruse, A. J.; Thomassen, P. L.; Riisager, A.; Mossin, S.; Fehrmann, R., Absorption and Oxidation of Nitrogen Oxide in Ionic Liquids. *Chemistry-a European Journal* **2016,** *22* (33), 11745-11755.
29. Hu, Z. H.; Margulis, C. J., Room-temperature ionic liquids: Slow dynamics, viscosity, and the red edge effect. *Accounts Chem. Res.* **2007,** *40* (11), 1097-1105.
30. Santiago, R.; Lemus, J.; Moreno, D.; Moya, C.; Larriba, M.; Alonso-Morales, N.; Gilarranz, M. A.; Rodríguez, J. J.; Palomar, J., From kinetics to equilibrium control in CO2 capture columns using Encapsulated Ionic Liquids (ENILs). *Chemical Engineering Journal* **2018,** *348*, 661-668.
31. Palomar, J.; Lemus, J.; Alonso-Morales, N.; Bedia, J.; Gilarranz, M. A.; Rodriguez, J. J., Encapsulated ionic liquids (ENILs): from continuous to discrete liquid phase. *Chemical Communications* **2012,** *48* (80), 10046-10048.
32. Lemus, J.; Palomar, J.; A. Gilarranz, M.; J. Rodriguez, J., Characterization of Supported Ionic Liquid Phase (SILP) materials prepared from different supports. *Adsorption* **2011,** *17*, 561-571.
33. Thomassen, P.; Kunov-Kruse, A. J.; Mossin, S.; Kolding, H.; Kegns, S.; Riisager, A.; Fehrmann, R., Separation of Flue Gas Components by SILP (Supported Ionic Liquid-Phase) Absorbers. In *Molten Salts and Ionic Liquids 18*, Reichert, W. M.; Mantz, R. A.; Trulove, P. C.; Ispas, A.; Fox, D. M.; Mizuhata, M.; DeLong, H. C.; Bund, A., Eds. 2012; Vol. 50, pp 433-442.
34. Mehnert, C. P.; Cook, R. A.; Dispenziere, N. C.; Afeworki, M., Supported Ionic Liquid Catalysis − A New Concept for Homogeneous Hydroformylation Catalysis. *Journal of the American Chemical Society* **2002,** *124* (44), 12932-12933.
35. Riisager, A.; Fehrmann, R.; Haumann, M.; Wasserscheid, P., Supported Ionic Liquid Phase (SILP) catalysis: An innovative concept for homogeneous catalysis in continuous fixed-bed reactors. *European Journal of Inorganic Chemistry* **2006,** (4), 695-706.
36. Fehrmann, R.; Riisager, A.; Haumann, M., *Supported Ionic Liquids: Fundamentals and Applications*. 2014; p 1-474.
37. Romanos, G. E.; Schulz, P. S.; Bahlmann, M.; Wasserscheid, P.; Sapalidis, A.; Katsaros, F. K.; Athanasekou, C. P.; Beltsios, K.; Kanellopoulos, N. K., CO2 Capture by Novel Supported Ionic Liquid Phase Systems Consisting of Silica Nanoparticles Encapsulating Amine-Functionalized Ionic Liquids. *The Journal of Physical Chemistry C* **2014,** *118* (42), 24437-24451.
38. Riisager, A.; Jørgensen, B.; Wasserscheid, P.; Fehrmann, R., First application of supported ionic liquid phase (SILP) catalysis for continuous methanol carbonylation. *Chemical Communications* **2006,** (9), 994-996.
39. Wang, H. B.; Hu, Y.-L.; Li, D.-J., Facile and efficient Suzuki–Miyaura coupling reaction of aryl halides catalyzed by Pd2(dba)3 in ionic liquid/supercritical carbon dioxide biphasic system. *J. Mol. Liq.* **2016,** *218*, 429-433.
40. Hu, Y. L.; Wu, Y. P.; Lu, M., Co (II)-C12 alkyl carbon chain multi-functional ionic liquid immobilized on nano-SiO2 nano-SiO2@CoCl3-C12IL as an efficient cooperative catalyst for C–H activation by direct acylation of aryl halides with aldehydes. *Appl. Organomet. Chem.* **2018,** *32* (2), e4096.

641 41. Yao, N.; Lu, M.; Liu, X. B.; Tan, J.; Hu, Y. L., Copper-doped mesoporous silica
642 supported dual acidic ionic liquid as an efficient and cooperative reusability catalyst for
643 Biginelli reaction. *J. Mol. Liq.* **2018,** *262*, 328-335.
644 42. Hu, Y. L.; Zhang, R. L.; Fang, D., Quaternary phosphonium cationic ionic
645 liquid/porous metal–organic framework as an efficient catalytic system for cycloaddition
646 of carbon dioxide into cyclic carbonates. *Environmental Chemistry Letters* **2019,** *17* (1),
647 501-508.
648 43. Jin, T.; Dong, F.; Liu, Y.; Hu, Y. L., Novel and effective strategy of dual bis
649 (trifluoromethylsulfonyl) imide imidazolium ionic liquid immobilized on periodic
650 mesoporous organosilica for greener cycloaddition of carbon dioxide to epoxides. *New J.*
651 *Chem.* **2019,** *43* (6), 2583-2590.
652 44. Lemus, J.; Bedia, J.; Moya, C.; Alonso-Morales, N.; A Gilarranz, M.; Palomar,
653 J.; J Rodriguez, J., Ammonia Capture from Gas Phase by Encapsulated Ionic Liquids
654 (ENILs). *RSC Advances* **2016,** *6*, 61650-61660.
655 45. Lemus, J.; Da Silva, F. A. F.; Palomar, J.; Carvalho, P. J.; Coutinho, J. A. P.,
656 Solubility of carbon dioxide in encapsulated ionic liquids. *Separation and Purification*
657 *Technology* **2018,** *196*, 41-46.
658 46. Moya, C.; Alonso-Morales, N.; Gilarranz, M. A.; Rodriguez, J. J.; Palomar, J.,
659 Encapsulated Ionic Liquids for CO2 Capture: Using 1-Butyl-methylimidazolium Acetate
660 for Quick and Reversible CO2 Chemical Absorption. *Chemphyschem* **2016,** *17* (23),
661 3891-3899.
662 47. Moya, C.; Alonso-Morales, N.; de Riva, J.; Morales-Collazo, O.; Brennecke, J.
663 F.; Palomar, J., Encapsulation of Ionic Liquids with an Aprotic Heterocyclic Anion
664 (AHA-IL) for CO2 Capture: Preserving the Favorable Thermodynamics and Enhancing
665 the Kinetics of Absorption. *The Journal of Physical Chemistry B* **2018,** *122* (9), 2616-
666 2626.
667 48. Santiago, R.; Lemus, J.; Moya, C.; Moreno, D.; Alonso-Morales, N.; Palomar,
668 J., Encapsulated Ionic Liquids to Enable the Practical Application of Amino Acid-Based
669 Ionic Liquids in CO2 Capture. *ACS Sustainable Chemistry & Engineering* **2018,** *6* (11),
670 14178-14187.
671 49. Buchel, G.; Unger, K. K.; Matsumoto, A.; Tsutsumi, K., A novel pathway for
672 synthesis of submicrometer-size solid core/mesoporous shell silica spheres. *Advanced*
673 *Materials* **1998,** *10* (13), 1036-1038.
674 50. Alonso-Morales, N.; Gilarranz, M. A.; Palomar, J.; Lemus, J.; Heras, F.;
675 Rodriguez, J. J., Preparation of hollow submicrocapsules with a mesoporous carbon shell.
676 *Carbon* **2013,** *59*, 430-438.
677 51. Alonso-Morales, N.; Ruiz-Garcia, C.; Palomar, J.; Heras, F.; Calvo, L.;
678 Rodriguez, J. J.; Gilarranz, M. A., Hollow Nitrogen- or Boron-Doped Carbon
679 Submicrospheres with a Porous Shell: Preparation and Application as Supports for
680 Hydrodechlorination Catalysts. *Industrial & Engineering Chemistry Research* **2017,** *56*
681 (27), 7665-7674.
682 52. Baukal, C. E.; Eleazer, P. B., Quantifying NOx for Industrial Combustion
683 Processes. *Journal of the Air & Waste Management Association* **1998,** *48* (1), 52-58.
684 53. Sousa, J. P. S.; Pereira, M. F. R.; Figueiredo, J. L., NO oxidation over nitrogen
685 doped carbon xerogels. *Applied Catalysis B: Environmental* **2012,** *125*, 398-408.
686 54. Kunov-Kruse, A. J.; Thomassen, P.; Mossin, S. L.; Riisager, A.; Fehrmann, R.,
687 Absorption and oxidation of NO in 1-butyl-3-methylimidazolium based ionic liquids -
688 mechanism of reaction. *Abstracts of Papers of the American Chemical Society* **2014,** *247*.

55. Mochida, I.; Kisamori, S.; Hironaka, M.; Kawano, S.; Matsumura, Y.; Yoshikawa, M., Oxidation of NO into NO2 over Active Carbon Fibers. *Energy & Fuels* **1994,** *8* (6), 1341-1344.
56. Mochida, I.; Kawabuchi, Y.; Kawano, S.; Matsumura, Y.; Yoshikawa, M., High catalytic activity of pitch-based activated carbon fibres of moderate surface area for oxidation of NO to NO2 at room temperature. *Fuel* **1997,** *76* (6), 543-548.
57. Guo, Z.; Xie, Y.; Hong, I.; Kim, J., *Catalytic oxidation of NO to NO2 on activated carbon*. 2001; Vol. 42, p 2005-2018.
58. Ruggeri, M. P.; Nova, I.; Tronconi, E., Experimental Study of the NO Oxidation to NO2 Over Metal Promoted Zeolites Aimed at the Identification of the Standard SCR Rate Determining Step. *Top. Catal.* **2013,** *56* (1), 109-113.
59. Atkins, P.; de Paula, J., *Atkins' Physical Chemistry*. 9th ed.; OUP Oxford: 2010.
60. Hubbe, M.; D Smith, R.; Zou, X.; Katuscak, S.; Potthast, A.; Ahn, K., *Deacidification of Acidic Books and Paper by Means of Non-aqueous Dispersions of Alkaline Particles: A Review Focusing on Completeness of the Reaction*. 2017; Vol. 12, p 4410-4477.
61. Lyon, R. K.; Cole, J. A.; Kramlich, J. C.; Chen, S. L., The selective reduction of SO3 to SO2 and the oxidation of NO to NO2 by methanol. *Combustion and Flame - COMBUST FLAME* **1990,** *81* (1), 30-39.
62. Zamansky, V. M.; Ho, L. O. C.; Maly, P. M.; Seeker, W. R., Oxidation of NO to NO2 by Hydrogen Peroxide and its Mixtures with Methanol in Natural Gas and Coal Combustion Gases. *Combust. Sci. Technol.* **1996,** *120* (1-6), 255-272.
63. Rasmussen, C. L.; Wassard, K. H.; Dam-Johansen, K.; Glarborg, P., Methanol oxidation in a flow reactor: Implications for the branching ratio of the CH3OH+ OH reaction. *International Journal of Chemical Kinetics* **2008,** *40* (7), 423-441.
64. Taylor, P.; Cheng, L.; Dellinger, B., The influence of nitric oxide on the oxidation of methanol and ethanol. *Combustion and Flame - COMBUST FLAME* **1998,** *115*, 561-567.
65. Alzueta, M. U.; Bilbao, R.; Finestra, M., Methanol Oxidation and Its Interaction with Nitric Oxide. *Energy & Fuels* **2001,** *15* (3), 724-729.
66. Xiao, C.-X.; Yan, N.; Zou, M.; Hou, S.-C.; Kou, Y.; Liu, W.; Zhang, S., NO2-catalyzed deep oxidation of methanol: Experimental and theoretical studies. *Journal of Molecular Catalysis A: Chemical* **2006,** *252* (1), 202-211.
67. Artioli, N.; Lobo, R. F.; Iglesia, E., Catalysis by Confinement: Enthalpic Stabilization of NO Oxidation Transition States by Micropororous and Mesoporous Siliceous Materials. *The Journal of Physical Chemistry C* **2013,** *117* (40), 20666-20674.
68. Loiland, J. A.; Lobo, R. F., Low temperature catalytic NO oxidation over microporous materials. *Journal of Catalysis* **2014,** *311*, 412-423.